The search for the origin of the quantum conditions under the paradigm of absolute space

Abstract

This study deals with the physical (not the mathematical) origin of the quantum conditions. The assumption of an absolute space together with the speed of 369.5 km/s of the sun leads to cycloidal or helical orbits of the electron around the proton. This kind of orbits is a previously unnoticed fact and not compatible with the model of a closed circular standing wave. It is the aim of this study to search for alternative models. The Alternating Field model (AFM) assumes the existence of alternating fields for both the proton and the electron. The Higgs-field provides the energy requirements. By Puthoff's effect, adapted for the electrostatic field, the electron changes its Compton frequency according to its position in the field. The interference of the alternating fields of the proton and the electron causes beats that are integer multiples of the orbital frequencies when the electron moves on Bohr's orbits.

Important results of this study are: The electrostatic Schwarzschild-radius is exactly half the value of the classical electron radius. Bohr's first three principal quantum numbers, 1, 2, 3, are reproduced as 1.000052, 2.000214, and 3.000685. A two-dimensional simulation shows that the AFM causes orbits with ribbon shape. A formula, using only the orbital frequencies of the two innermost circular orbits, can predict the shortest wavelength of the Lyman series.

The AFM is still incomplete. E.g., it does not prevent illegal orbits, but only indicates them. Also, the AFM does not use the magnetic core field of the proton. On the other hand, the model has produced results showing that Newton's absolute space and the QM are compatible.

Keywords: Absolute space, spherical harmonics, cycloidal orbits, alternating field, Higg's field

1. Introduction

The assumption of an absolute space together with the speed of 369.5 km/s of the sun leads to cycloidal or helical orbits of the electron around the proton. This previously unnoticed fact makes using Legendre's spherical harmonics for the description of the quantum conditions in quantum mechanics a purely mathematical formalism. Here, we are looking for the physical bases. Cycloid and helix are curves composed of a circular and a translational motion. Therefore, the decomposition of total energy into rotational and translational energy is possible. Also, the decomposition of the momentum and angular momentum is possible for both curves. This way, we can be sure that the results of the QM remain valid.

The electron is surrounded by electromagnetic fields. One can specify here:

- The DeBroglie-wave, which is connected with the momentum of the electron [1].

- The Compton-wave, which is connected with the mass of the electron [2]. The energy for this as well as for the synchrotron radiation [3], which is, here, very low, comes from the Higgs field.
- Dirac's zitterbewegung of the electron [4, 5].

The quark-model of the baryons [6] allows one to derive a model in which the charged quarks orbit around the center of mass, and could, this way, cause an alternating field. As in the case of the electron, another possible source could be a quark itself. In addition, there are magnetic fields. Here, the magnetic field of the proton is of particular importance, since it could provide a relatively stable spatial orientation. Both electric alternating fields, that of the proton and that of the electron, would interfere with each other. Additionally, the orbital movement of the electron would interfere with the stably spatially oriented magnetic field of the proton. Together, these effects could be the causes of the quantum conditions in Bohr's atomic model.

In Bohr's first atomic model [7, 8], the electrons move on circular orbits around a fixed nucleus. But in the improved model of Bohr and Sommerfeld [9], the movement of the nucleus and elliptical orbits are considered. Later, quantum mechanics (QM) replaced the Bohr-Sommerfeld atomic model. This theory considers the quantum conditions the cause of the existence of a radiation-free standing wave (DeBroglie-wave), which is connected with the movement of the electron [1, 2, 10]. One solves the Schrödinger equation [11] (or the Klein-Gordon equation, or the Dirac equation, respectively) [12] by calculating the eigenvalues and eigenfunctions of the angular momentum operator. Here, the quantum conditions appear because only integer parameters (principal quantum number *n*, orbital angular momentum quantum number *l*, magnetic quantum number *m*) lead to the eigenfunctions in the form of Legendre's spherical harmonics [2, 12]. As an example, consider the azimuthal equation:

$$\frac{\partial^2}{\partial\varphi^2}\Phi_m(\varphi) = -m^2\,\Phi_m(\varphi). \qquad (1.1)$$

The solution is $\Phi_m(\varphi) = Ae^{im\varphi}$. However, solutions that fulfill the condition $\Phi_m(\varphi + m2\pi) = \Phi_m(\varphi)$ can be found only for integer values of *m*. This is precisely the condition under which the azimuthal wave without a phase jump assumes its original value after one complete revolution of the sphere.

However, assuming the existence of the absolute space in which waves propagate, and furthermore, assuming that our solar system moves with a speed of 369.5 km/s through this space, then also all protons (in Fig. 1 labeled by ***P***) move at this speed. So, in the special case of a circular orbit of the electron (in Fig. 1 labeled by ***e***) and a relative speed of the electron of about 2200 km/s, the actual orbit of the electron in the absolute space is not a closed circle, but a) a helix, or b) a helix with an inclined axis, or c) a cycloid, depending on the orientation of the electron orbit to the direction of the speed of the moving atom in absolute space.

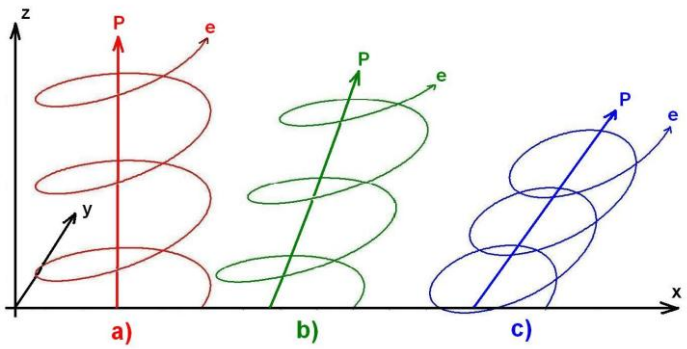

Fig. 1: Orbits of the electron in the absolute space

a) Helix, b) inclined helix, c) cycloid

In Case a), the direction of translation, *P*, is perpendicular to the plane of the orbit of the electron. In Case b), the direction of translation, *P*, is inclined to the plane of the orbit. In Case c), the case of the cycloid, the direction of translation, *P*, lies in the plane of the orbit. Cases a) and c) are point events with probability zero. Case b) is true for all angles unequal to 0° and 90° between direction P and the plane of the orbit of the electron, and is, therefore, the general case. Only in the case of the cycloid, the orbit of the electron crosses its old course again. But in the case of the cycloid as well, the courses just cross, and, thus, are neither a directional nor a phase-accurate continuation of the old orbit. This way, under the assumption of the absolute space, one has a problem with Legendre's spherical harmonics. On top of that, even in quantum mechanics, the origin of the quantum conditions is nowhere discussed. One is satisfied with the fact that the physical measurements, consistent with mathematics, prescribe integer quantum numbers.

Since both the cycloid and the helix are curves that are composed of a translational and a rotational movement, the decomposition of the total energy into rotational and translational energy is possible. Also, a clean separation is given of momentum and rotational momentum for both curves. So, it is very well possible that the results of the QM retain their validity unaltered (except for tiny relativistic corrections). The only element that would change is the physical foundation of the quantum conditions.

We would like to add a few thoughts at this point:

- Heisenberg's uncertainty principle [2] $\Delta p \Delta q \approx h/(2\pi)$ describes the impossibility to measure, at the same time, with any precision, the momentum coordinate $\boldsymbol{p}$ and the location coordinate $\boldsymbol{q}$ of a particle. Any measuring process, no matter how fine, causes interferences, which cause the above-mentioned uncertainty. However, we consider the often-used inversion of Heisenberg's uncertainty principle to be speculation, e.g., that in the case of an exact given momentum $\boldsymbol{p}$ the location $\boldsymbol{q}$ of the particle becomes indefinite in the sense that the electron is everywhere. One should prefer to say that, in this case, the exact location at a certain point in time is not determinable. Scattering experiments of electrons with electrons have shown that the electrons are almost point-like with an extremely small diameter, which researchers have not yet been able to determine more precisely, and that at relativistic velocities close to the speed of light. Therefore, the electron has a well-defined position coordinate and a well-defined

velocity – but they cannot be measured both at the same time more accurately than Heisenberg's uncertainty principle allows.

- QM calculates, for the electrons of an atom, probabilities of residence in preferred orbitals. One should interpret this statement to mean that an electron is located successively over the course of time in different space segments, overall, however, with the calculated probability. Therefore, the probability of residence is a temporal average. However, we fully agree with QM in that one should exclude the predictability of an electron orbit, since that would require the actual exact path parameters and initial values, which, according to Heisenberg, is impossible. In addition, it would also require well-defined forces when integrating. The latter is, according to our model, also questionable. However, in simulations, one should definitely be allowed to use well-defined electron orbits, even if we cannot verify them in experiments.
- Although the accuracy of many results of the QM is surprisingly high (up to 11 digits), the question of absolute accuracy still remains. Although we also assume a constant speed of light, we predicted in [13] a seasonal variation of this speed of ±36.9 m/s for earth-based measuring devices. The reason is the orbital movement of the earth around the sun, and the associated varying dilation of time. So, if the important natural constant $\boldsymbol{c}$ is only constant to 7 instead of 10 digits, this also applies to all calculated constants that contain the quantity $\boldsymbol{c}$. Another example is the 10-digit accuracy of the calculated energy levels in the hydrogen atom. However, these are relative accuracies based on an imprecise base value, because the measured wavelength of the emitted radiation is known only with 4 or 5 digits, however, with a maximum of 7 digits. Even if one compares the frequencies electronically with a frequency standard, it remains the inaccuracy of 10^{-7} of the time standard caused by the varying dilation of time during the orbital movement of the earth around the sun.

Despite our mild criticism – QM is one of the best verified theories in physics. It describes the processes in the atom with uncommon precision. If we nevertheless question the origin of the quantum conditions, we must look for answers that are largely compatible with the results of QM.

2. Basics of Membrane Theory

The assumption of an absolute space in Newton's sense is a direct or indirect conclusion from membrane theories [14, 15. 16]. We also support the existence of a supermembrane (cosmic membrane), and have published, in the past, numerous articles, dating back to 1995, on the theory of the cosmic membrane (CM) and the associated absolute space. One can find a detailed summary of essential details in [17]. Here, we repeat the main results as they are relevant to this article, in abbreviated form.

Our cosmos is an expanding membrane. The three-dimensional membrane (the 4^{th} dimension, the thickness of the membrane, is extremely small) expands as the surface of a 4D-balloon inflated in 4D hyperspace. A homogeneous vector field, which has properties of the Higgs

field, acts parallel to the direction of expansion, i.e., perpendicular to the membrane. The vector field can easily permeate the undisturbed membrane. In the case of embedded matter, the vector field exerts pressure on the matter which deforms the membrane. This pressure force works from the 4th dimension, *w*. In the case of spherical masses, e.g., the sun or the earth, one obtains a gravitational funnel with spherical symmetry. Fig. 2.a shows a projection of the 4D-space (*x, y, z, w*) with two gravitational funnels in a simulated membrane. The curvature and spatial depth of the funnels are greatly exaggerated.

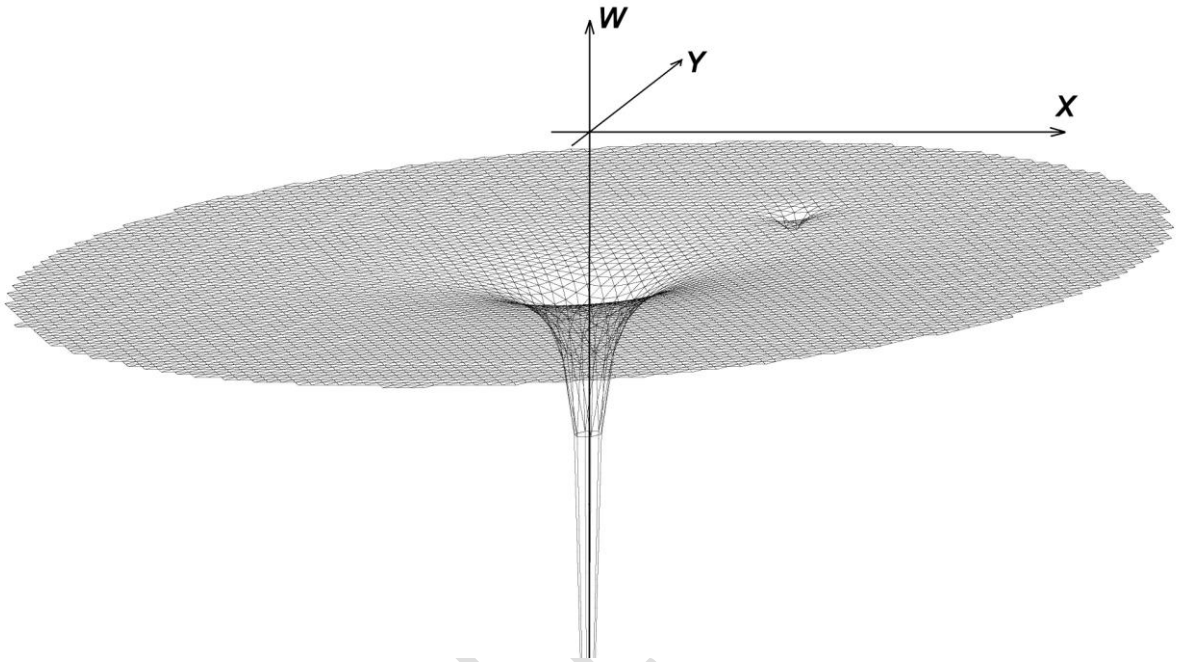

Fig. 2.a: Two gravitational funnels of the 3D-membran in 4D-space.
Shown is only the x-y-plane of the 3D-grid.

The tension of the undisturbed membrane is F_0 with unit [N/m^2]. In the case of spherical masses, the ODE of curvature of the membrane is

$$w'' = -2w'/r\,. \qquad (2.1)$$

Each function $w(r)=C_1+C_2/r$ is a solution of ODE (2.1). Fig. 2.b shows the decomposition of the pressure force *F* acting from the 4th dimension, *w*, on a small mass *m*. The horizontal component F_{DH} is the downhill force, acting in x-, y-, or z-direction. The vertical component is F_V acting in negative w-direction.

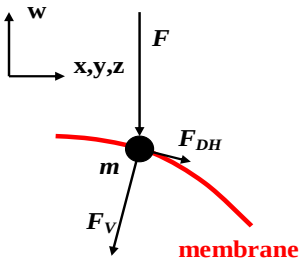

Fig. 2.b: Decomposition of pressure force *F*

For F_{DH}, we find the relation $F_{DH}=m\,A_{VFH}\,sin(\alpha)$. The quantity A_{VFH} is the horizontal vector field acceleration, and α is the rise angle of the membrane in the distance r from the center of the funnel. In the case of small angles α, the relation $F_{DH} = m\,A_{VFH}\,w'(r)$, or $F_{DH} = m\,g_S(r)$ is obtained with gravity acceleration $g_S(r)$ in the distance r from the center of the funnel. This corresponds to Newton's universal law of gravitation.

We apply the relation $F_{DH} = m\,A_{VFH}\,w'(r)$ to the solar system. One obtains the gravity acceleration at the edge of sun, i.e., $g_{RS} = A_{VFH}\,W'_{RS}$. By Newton is $g_{RS} = -\gamma M_S / R_S^2$. If the numerical value of the slope of the membrane, W'_{RS}, at the edge of sun were known, one could calculate the horizontal vector field acceleration A_{VFH}. For $r\to\infty$, the value w of the depth of space is set equal to zero, i.e., $w(r\to\infty) = 0$. This way, one can write the radial function of the curvature of space, $w(r)$, in the form $w(r) = -W_{RS}R_S / r$.

With $w'(r) = W_{RS}\,R_S / r^2$, one obtains the relation $W'_{RS} = W_{RS} / R_s$. Here, W'_{RS} is the slope of the membrane at the edge of sun.

Now, we make the connection to Einstein's theory of gravitation using Feynman's radius of excess, $r_{Ex}=a/3=491$[m] [2], and formally equate Feynman's radius of excess to the path extension d_{SR} which appears while traversing the path from the edge of sun to its center on the curved membrane. The direct path would extend from the edge of the sun at constant altitude w to the w-axis, going through the center. Here, the quantity a is the Schwarzschild radius of the sun. One can show that the geometrical path extension dS outside the sun equals the path extension within the sun. One can calculate the path extension dS outside the sun without having to make assumptions about the density within the sun.

$$dS = \int_{RS}^{\infty} \frac{1}{2} w'^2(r)\,dr = \int_{RS}^{\infty} \frac{W_{RS}^2\,R_S^2}{2r^4}\,dr = \frac{W_{RS}^2}{6R_S}. \qquad (2.2)$$

With Feynman's value of his radius of excess, $r_{EX} = dS = 491$ [m], and the solar radius of $R_S=6.958\times10^8$ [m], we obtain, in our cosmic membrane model, the value $W_{RS} = 1.432\times10^6$ [m] for the depth of space at the edge of the sun. With the gravity acceleration $g_{RS} = \gamma M_S / R_S^2 = 273.65$ [m/s^2] at the edge of the sun and the above values of R_S and W_{RS}, we obtain the value of the horizontal vector field acceleration, $A_{VFH} = g_{RS} / W'_{RS} = 1.330\times10^5$ [m/s^2].

The membrane holds the sun. The force $F = M_S A_{VFV}$ acts in the negative w-direction on the mass of the sun. It must be compensated by the sum of the vertically in positive w-direction acting components $F_{0w} = F_0 \sin(\alpha)$ of the membrane tension, which pull, at the edge of the sun, with the surface $4\pi R_S^2$. Here, A_{VFV} is the vertical vector field acceleration. For small angles α, one obtains, with $\sin(\alpha) \approx W_{RS} / R_S$, the relation

$$F_0 = \frac{M_S\,A_{VFV}}{4\pi\,R_S\,W_{RS}}. \qquad (2.3)$$

Unfortunately, according to Chandrasekhar [18], the simultaneous calculation of F_0 and A_{VFV} succeeds only iteratively by the solution of a system of difference equations set up in the calculation of the gravitational energy E_G of the sun. Hereby, the quantities F_0 and A_{VFV} are two parameters which control the compliance with the two constraints $w'(r\to\infty)=0$ and $E_G=E_{G,Ch}$ and, additionally, the constraint given by Eq. (2.3). Here, $E_{G,Ch}$ is the value of the

gravitational energy given by Chandrasekhar. The fit of the parameters gave the values F_0 =1.820×10^{19} [N/m^2] and A_{VFV}=1.148×10^5 [m/s^2]. Evidently, the two vector field accelerations, A_{VFH} and A_{VFV}, differ.

At this juncture, one can only speculate about the value of the speed V_E of expansion of the cosmic membrane in the direction of the 4th dimension. However, if $V_E < c$, the curvature of space should be visible by a disproportionate increase in the density of galaxies with increasing distance. However, since there is no evidence of this, we assume $V_E \geq c$.

In the simplest case, one can imagine the homogeneous vector field (Higgs field) as a gas flow that hits the membrane with speed $V_E \geq c$. So, the sun with its mass M_S=1.985×10^{30} [kg] is exposed to a force of $F_S = M_S A_{VFV}$ = 2.279×10^{35} [N]. Under the assumption of $V_E = c$, this creates a braking power (the power loss of the homogeneous vector field when crossing the sun) of $P_{BS} = M_S A_{VFV} c$ = 6.832×10^{43} [W]. Measured against this, the radiant power of ca. P_{RS} =4×10^{25} [W] of the sun is modest.

One kilogram of matter creates a power loss of the homogeneous vector field (or braking power) of ca. 3.4×10^{10} [kW]. This is the power of ca. 34.000 power plants, each of them with a power of one million kW. However, one can assume that the main part of the energy brought in by the vector field does not remain in the matter, just as a storm sweeping through the forest does not cause the forest to glow. The main part of the energy will leave the membrane unused, but a fraction of it could well keep the atom going, despite the constant loss of energy due to the radiation of an alternating electric field and a certain synchrotron radiation of the orbiting electrons.

We make the calculation for the proton. It has the mass m_P =1.673×10^{-27} [kg]. The braking power in the vector field is $P_{BP} = m_P A_{VFV} c$ = 5.758×10 $^{-14}$ [W]. Compared with the radiation energy $E_{PH} = h \nu \sim 10^{-18}$ [Ws] of a typical photon emitted from the hydrogen atom with a radiation frequency of ca. ν=10^{15} [Hz], the braking energy per second is 4 to 5 orders of magnitude higher. That means, it is high enough to supply the energy for an alternating field around the proton, at least theoretically.

3. Alternating field model

We want to try to replace the loss of the justification of the quantum conditions by a standing wave with another justification. Hereby, the most important condition is that the results of QM remain largely undamaged.

Our model of the new quantification is the alternating field model (AFM). A special electromagnetic [12] alternating field of the proton spreads in space. The space is thereby *ribbed*. The electron has its own alternating field with similar frequency, which interacts with the alternating field of the proton. In addition, the magnetic field of the proton ensures a sufficiently stable spatial orientation. Hereby, it is assumed that a precession or change in the magnetic field proceeds much slower than the time needed for an orbit of the electron. However, the magnetic field is not used in our previous model. Our guess is that it could play an important role as space normal, and when emitting or capturing a photon. Fig. 3. shows the instantaneous image of the alternating electric field of the proton and its magnetic field, plus a circular orbit of the electron.

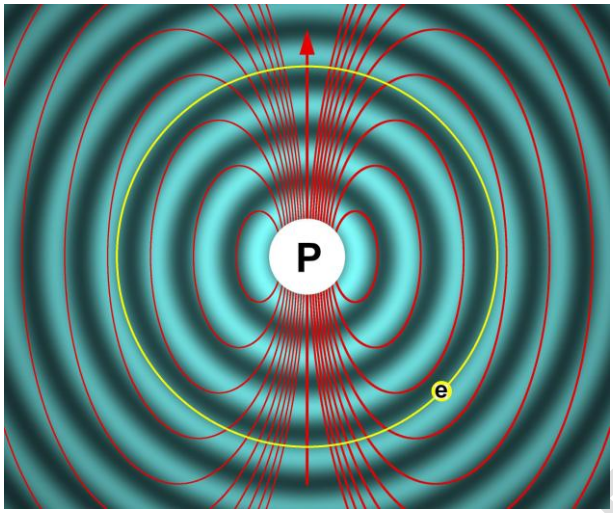

Fig. 3: Alternating electric field of the proton and its magnetic field

Because of the different speeds of the electron on its different orbits around the proton, the mass of the electron changes. The Compton frequency ω_C of the electron is coupled to the mass via the relation $\omega_C = m_e(v)c^2/\hbar$. The frequency increases due to the relativistic mass increase of the electron. However, due to time dilation $\omega(v) = \omega_0\sqrt{1-v^2/c^2}$, it would be revoked immediately. To solve this dilemma, one result may help us that Puthoff [20] published in 2002 in his *Polarizable-vacuum approach to GR*. The authors derived the same result in 2016 from Einstein's momentum-energy relation $E^2 = (m_0c^2)^2 + (pc)^2$, and used it for the calculation of the geodetic precession [21]. Puthoff's result was: When a small mass is in free fall in the gravitational field of a massive body, this small mass has a relativistic increase in mass of $dm(r) = a/r + 2a/r$. Here, the quantity a is the Schwarzschild radius and r the distance of the small mass from the central mass. The first term, a/r, is the known relativistic increase of mass with speed. The additional term, $2a/r$, is probably caused by a change in the membrane properties in the gravitational funnel.

We would like to transfer this important result to the electrostatic conditions in the hydrogen atom. The nucleus of the hydrogen atom, the proton, is surrounded by an electrostatic field within which the electron moves. This is reminiscent of the sun, in whose gravitational field the planets orbit. Both the gravitational field of a central mass and the electrostatic field of a single charge have a conservative potential that can be represented by very similar formulas. The potential of gravity is $P_G(r) = \gamma Mm/r$ [Nm], where γ is the gravitational constant, M the central mass, m a small mass of 1 [kg], and r the distance between the small mass and the central mass. For comparison: The potential of an electric charge is $P_e(r) = (1/(4\pi\varepsilon_0))eE/r$ [VAs =Nm], where ε_0 is the dielectric constant, e the elementary charge, and E=1 [As] the unit charge. One can, therefore, suspect that, based on this similarity, the same relativistic increase in mass appears in the electrostatic field as in the gravitational field. However, one must use the electrostatic equivalent a_{el} instead the Schwarzschild radius $a = \gamma M/c^2$ in Eq. (3.1) of the relativistic increase of mass, i.e.,

$$dm(r) = a_{el}/r + 2\,a_{el}/r\,. \qquad (3.1)$$

The following estimate provides the numerical value of the electrostatic Schwarzschild radius a_{el}. The relativistic increase in mass the relation $1 + a_{el}/r = 1/\sqrt{1 - v^2/c^2}$ is used. With this and in the case of small velocities v, one finds $a_{el}/r = v^2/(2c^2)$. One obtains the value $a_{el} = (r\,v^2)/(2\,c^2) = 1.408970\times10^{-15}$ [m] using the radius $r = a_0 = 5.291772\times10^{-11}$ [m] of Bohr's innermost circular orbit, and using the velocity $v_0 = 2.187691\times10^{6}$ [m/s] of the electron on this orbit. This is half the classical electron radius. In the literature, it is given as $R_{e,cl} = 2.8179403262\times10^{-15}$ [m].

In the following study, we will focus on the Compton circular frequency of the electron,

$$\omega_{C0} = m_e c^2/\hbar = 7.763441\times10^{20}\ \text{[rad/s]}. \quad (3.2)$$

Our reasons include: (1) The theory of the zitterbewegung of the electron [4, 5] has a suspicious side. If one calculates the speed of the electron on its trembling course, one obtains a speed which 4π times the speed of light. The simple straight speed of the electron is not even taken into account here. (2) The DeBroglie frequency of the electron is too small to expect a corresponding frequency from the proton.

Our quantum condition is that the orbital speed v of the electron on its orbit around the moving proton can only assume values where the relativistic increase of mass of the electron leads to a Compton circular frequency of the electron ω_{Cv}. This frequency differs only by an integer multiple of the orbital frequency ω_0 from the Compton circular frequency ω_{C0} of the resting electron.

The orbital frequency ω_0 is the circular frequency with which, in Bohr's atomic model, the electron orbits the nucleus on the innermost circular path. The value is $\omega_0 = 4.134137\times10^{16}$ [rad/s].

Table 1 shows Bohr's orbital speeds for the 3 innermost orbits and their radii r_i. The relativistic mass and its increase given by Puthoff's effect obeys the equation $m_e(r_i) = m_{e0}(1 + 2\,a_{el}/r_i)$. Here, m_{e0} is the rest mass of the electron. Now, the Compton circular frequency of the electron, ω_{Ci}, is calculated using the formula $\omega_{Ci} = m_e(r_i)c^2/\hbar$. Then, the differences $\omega_{Ci} - \omega_{C0}$ between ω_{Ci} and the Compton circular frequency ω_{C0} of the resting electron are calculated. Then, we compare these differences with the orbital frequencies ω_{0i} of Bohr's three innermost orbits with i=1, 2, 3, and $\omega_{0i} = v_i/r_i$.

Table 1: Relativistic change of the Compton circular frequency depending on the speed of the electron on Bohr's three innermost circular orbits

Orbit	1	2	3
Radius [m]	5.291770×10^{-11}	2.116709×10^{-10}	4.762595×10^{-10}
Speed [m/s]	2.187633×10^{6}	1.093838×10^{6}	7.292283×10^{5}
Mass [kg]	9.109869×10^{-31}	9.109505×10^{-31}	9.109438×10^{-31}
ω_{Ci} [rad /s]	7.763854×10^{20}	7.763544×10^{20}	7.763487×10^{20}
$\omega_{Ci}-\omega_{C0}$ [rad /s]	4.134241×10^{16}	1.033638×10^{16}	4.594522×10^{15}
ω_{0i} [rad /s]	4.134027×10^{16}	5.167637×10^{15}	1.531157×10^{15}

$(\omega_{Ci}-\omega_{C0}) / \omega_{0i}$	1.000052	2.000214	3.000685

As one can see, the Compton circular frequency changes indeed to a first approximation by an integer multiple of the orbital frequency ω_{0i}. This suggests that a connection exists between the Compton frequency and the orbital frequencies.

Unfortunately, the ratios $(\omega_{Ci} - \omega_{C0}) / \omega_{0i}$ are not the exact integers, 1, 2, 3, but the slightly different values 1.000052, 2.000214, and 3.000685. The cause of this slight deviation, which increases with the principal quantum number n, still needs to be determined.

4. Interference of the alternating fields

In this section, we estimate the forces that occur when there is interference between the alternating field of the proton and the alternating field of the electron. The speed v_P of the proton in the absolute space is of the order $0.001c$, and can, therefore, be neglected in a first approximation when it comes to the propagation of the alternating fields.

In the simplest model, the proton radiates with the Compton circular frequency $\omega_{C0}=7.763441\times10^{20}$[rad/s]. The source of this radiation could be the Down quark. One could think of it as resting in the center of the proton. The electron is surrounded by an alternating field that changes its frequency with its relativistic mass (see Section 3). The two alternating fields overlap and interfere. This creates electrostatic attraction or repulsion. The movement of the electron in the magnetic field of the proton does not change the attraction or repulsion, but causes disturbances in the form of lateral deviations from the ideal circular orbit.

For a hydrogen atom resting in space, circular orbits are possible. Also, for the moving proton, but now in the moving coordinate system, the orbits of the electron may remain circular. The cycloid and helical curves are rolling curves in which a rotational movement is superimposed onto the translational movement. Both the rotational energy and the angular momentum can be separated cleanly from the translational energy and the momentum. In the case of uniform motion of the proton, they are independent of each other. This way, the mathematical basics of the QM remain preserved, but not the physical justification.

Here, the interference integral $\overline{F}$ is the dimensionless arithmetic mean of the product $\sin(\omega_{C0} t)\sin(\omega_{Ci} t)$ of the amplitudes of the interfering electric fields for the orbiting electron over one cycle, i.e.

$$\overline{F} = \frac{1}{T}\int_0^T \sin(\omega_{C0} t)\sin(\omega_{Ci} t)\,dt\,. \qquad (4.1)$$

Then, the force effect of the alternating fields on the electron is $f=f_0\,\overline{F}$ [N]. Here, the quantity $f_0 = -e^2/\left(4\pi\varepsilon_0 r^2\right)$ is a factor with the dimension of a force, and depends, moreover, on $1/r^2$. The quantity T is the orbital period, ω_{C0} the circular frequency of the alternating field of the proton, and ω_{Ci} the relativistically altered circular frequency of the alternating field of the electron on its orbit with radius r_i. The factor f_0 is negative. So, in this context, positive values of $\overline{F}$ mean a force acting in the direction of the proton, negative in the direction away from the proton, i.e., in the direction of the radius.

Fig. 4.a shows the interference integral $\overline{F}$ depending on the radius r of the circular orbit of an electron. The radius is given in units of radius a_0.

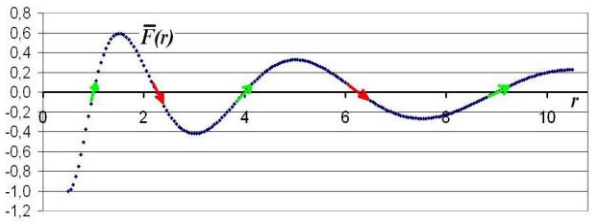

Fig. 4.a: Function $\overline{F}$ (r) with zero points for stable (green) and unstable (red) orbits

The radius r_i varies from 0.5 a_0 to 10 a_0. The parameters a_0, $a_1=4\ a_0$, and $a_2=9\ a_0$ are the radii of Bohr's innermost three circular orbits. In Fig. 4.a, they are marked by green arrows. The circular frequency of the alternating field of the electron, ω_{Ci}, is $\omega_{Ci}=\omega_{C0}\ (1+2a_e/r_i)$, due to Puthoff's relativistic increase in mass. We have normalized the values of the interference integral $\overline{F}$ displayed in Fig. 4.a so that the minimum value of the curve is exactly $\overline{F}$ (r)= –1, i.e., all calculated values have been divided by 0.10848154.

The disappearance of the interference integral $\overline{F}$ (r) on Bohr's circular orbits suggests that both electrical fields have exactly that constant part of the electrostatic field, which ensures the equilibrium between centrifugal force and force of attraction on Bohr's circular orbit, besides their alternating parts. Therefore, one can tentatively specify the following approach for the field of the proton at the location of the electron:

$$E_p(r,t)=\frac{e}{4\pi\varepsilon_0 r^2}\left(1+\beta_p \sin(\omega_{C0}\,t)\right), \qquad (4.2)$$

For the electron, we write

$$E_e(r_i,t)=-e\left(1+\beta_e \sin(\omega_{Ci}\,t)\right). \qquad (4.3)$$

In Equations 4.2 and 4.3, the factors β_p and β_e are still unknown dimensionless parameters from the interval [0, 1]. In Section 5, some remarks on these parameters will be given. The product $F=E_p(r,t)E_e(r_i,t)$, it describes the interaction of the two fields, contains four parts. $F_1=-e^2/4\pi\varepsilon_0 r^2$ is the electrostatic attraction between electron and proton; it depends only on the radius. It is directed from the electron to the proton. The parts $F_2=-(\beta_e e^2/(4\pi\varepsilon_0 r^2))\sin(\omega_{Ci}\,t)$ and $F_3=-(\beta_p e^2/(4\pi\varepsilon_0 r^2))\sin(\omega_{C0}\,t)$ oscillate for constant radii very quickly about the value $F=0$, so that the mean value $\overline{F}$ vanishes always after one vibration.

The part

$$F_4=-(\beta_p\,\beta_e e^2/(4\pi\varepsilon_0 r^2))\sin(\omega_{C0}\,t)\sin(\omega_{Ci}\,t) \qquad (4.4)$$

is the interfering part, i.e., the force produced by the alternating parts of the two fields. The arithmetic mean of this part is $\overline{F}_4=-(\beta_P\,\beta_e e^2/(4\pi\varepsilon_0 r^2))\,\overline{F}$. By our calculations, it vanishes on Bohr's circular orbits, but only if one integrates exactly one orbit.

However, between Bohr's circular orbits, there still exist other radii with a vanishing mean value $\overline{F}$ of the interference integral (in Fig. 4.a marked by red arrows). These orbits are, in contrast to Bohr's orbits, unstable. When an electron moves on a stable orbit and, caused by a small perturbation, moves to a somewhat smaller radius, the integral $\overline{F}$ assumes a negative value. This implies a force away from the proton, i.e., in the direction of the radius. When the electron moves on a radius that is too large, the integral $\overline{F}$ assumes a positive value, and that means a force in direction to the proton. So, in the case of small perturbations, the electron will be led back to Bohr's circular orbit.

In the cases of unstable orbits with $\overline{F}$ =0, the action is reversed. If the electron moves on a radius that is too large, the integral $\overline{F}$ assumes a negative value, and that means a force in the direction of the radius. In the case of a radius which is too small, $\overline{F}$ has a positive value, which implies a force in the direction of the proton. That means, each small perturbation will be amplified, and the electron will be derailed from its unstable orbit - theoretically. Here, *theoretically* means that, in our simulations, the electron will not be derailed from its unstable orbit, i.e., our model is still imperfect. This is a question that still needs to be clarified.

The function $F(t) = \sin(\omega_{C0}\, t)\sin(\omega_{Ci}\, t)$ is quickly oscillating. Fig. 4.b shows a short section, for small values of Time *t*, i.e., at the beginning.

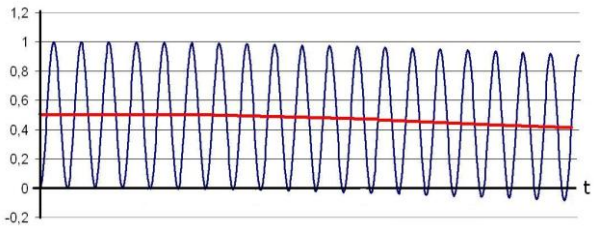

Fig. 4.b: Function F(t) with arithmetic mean (red)

The frequency is nearly exactly that of the zitterbewegung of the electron, because, by the multiplication of the two sine functions, the Compton frequency is doubled. Because of the mass of the electron, smoothing takes place, and one obtains a smoothed curve, i.e., a kind of average, starting at the value 0.5 (red curve in Fig. 4.b). Fig. 4.c shows the further course of the curve on the orbit of the electron. T_0 is the respective orbital period in the corresponding orbit (a_0, a_1, a_2). The smoothed curves, $\tilde{F}_{ai}(t)$, are cosine functions, and have the frequencies of the known DeBroglie-waves of the electron in Bohr's circular orbits.

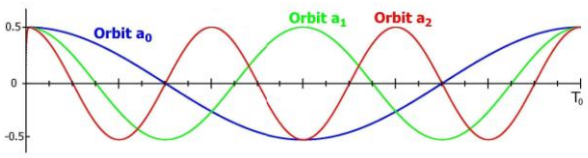

Fig. 4.c: DeBroglie-waves $\tilde{F}_{ai}(t)$ for the orbits a_0, a_1, a_2

$\tilde{F}_{a0}(t)$ is a cosine function for the orbit with radius a_0, $\tilde{F}_{a1}(t)$ is a cosine function for radius a_1, and $\tilde{F}_{a2}(t)$ for radius a_2. Each curve has the number *n* of wave trains for one orbital period that is posited in Bohr's theory and also in the QM.

DeBroglie matter waves on the i-th Bohr's circular orbit have the same frequency as the corresponding interference function $\tilde{F}_{ai}(t)$. However, the DeBroglie matter waves are not used in our model. The reason is that we cannot say clearly whether this kind of waves appears for free electrons as well. In other words, we do not know whether this wave is a feature of the electron, or whether this wave is just an artifact that appears only in the surrounding of protons. We think this is another question that still needs to be clarified.

5. Numerical simulations

5.1 Physical basics

The results of the integration of the function $\tilde{F}_{a0}(t)$ show that the maximum deflection of the electron caused by its zitterbewegung is of the order 10^{-18} [m], and not of the order of the Compton wavelength $\lambda_C = 2.426\times10^{-12}$ [m], as calculated by Breit and Schroedinger in their theory of Dirac's zitterbewegung of the electron [4, 5].

Consider Bohr's atomic model of the hydrogen atom with its circular orbits on which the electron rotates around the nucleus. Our simplified model uses only the conservative potential of the electrostatic attraction between proton and electron, i.e., the magnetic influences are neglected. So, one can calculate exactly the energies and parameters of the orbits.

We start with the energy E_w, which is emitted by the electron when it *falls* from infinite distance onto the innermost circular orbit in Bohr's model. This energy is known very exactly.

$$E_w = h R_H c = 2.178685785926\times10^{-18} \text{ [J]}. \qquad (5.1)$$

Here, h is the Planck constant $h=6.6260701102206\times10^{-34}$ [Nms], R_H is Rydbergs wave number per meter of the hydrogen atom, $R_H=1.096775834120630\times10^{7}$ [m^{-1}], and $c=299{,}792{,}456.224274$ [m/s] is the speed of light.

By equating the wave energy E_w with the kinetic energy $E_k=(\mu/2)v^2$, one obtains the orbital speed of the electron

$$v = \sqrt{2E_k/\mu} = 2.18766214\times10^{6} \text{ [m/s]}. \qquad (5.2)$$

Here, the quantity μ is the reduced mass of the electron, $\mu = (m_{er}\, m_p) / (m_{er}+m_p) = 9.10466757\times10^{-31}$ [kg], which takes in consideration the co-motion of the hydrogen nucleus. The quantity m_{er} is the relativistic mass of the electron with $m_{er}=9.109626255\times10^{-31}$ [kg], and m_p is the mass of the proton with $m_p=1.672621924\times10^{-27}$ [kg].

The orbital angular momentum on the innermost circular orbit is $J = \hbar$ with $\hbar = h / 2\pi$. So, the orbital radius r_0 using the relation $J=m_e v r$ can be calculated as

$$r_0 = \hbar/(m_e v) = 5.2917721085959\times10^{-11} \text{ [m]}. \qquad (5.3)$$

Coulomb's potential $E_C = e^2/(4\pi\varepsilon_0 r_{ep}^2)$ is, in Bohr's model, the sum of wave energy and kinetic energy, i.e., $E_C = E_w + E_k$. Therefore, using this equation, one can calculate the distance between proton and electron, r_{ep}, as

$$r_{ep} = \sqrt{e^2/(4\pi\varepsilon_0 E_C)} = 5.2946541583721\times10^{-11} \text{ [m]}. \qquad (5.4)$$

Here, e=1.602176634000×10^{-19} [As] is the charge of the electron or proton, respectively. The quantity ε_0 is the dielectric constant of the vacuum with ε_0=8.854187817000×10^{-12} [As/Vm]. With reference to the center of gravity theorem, the relationship between orbital radius r and distance proton-electron is determined to be r_{ep}= r (1+m_e/m_p). So, one can calculate the ratio m_p/m_e as $r/(r_{ep}-r) \sim m_p/m_e$ = 1836.114. This value deviates a little from the value m_p/m_e = 1836.152673. The theory explains this discrepancy by positing that there is a little difference between the location of the charge and the center of mass in the proton.

So, as defined in Bohr's model, our numbers match exactly. However, Bohr's atomic model cannot explain the fine structure of the lines emitted by the hydrogen atom. Therefore, Sommerfeld [9] and, later, QM extended Bohr's model. An important insight of QM is that there exists a spherical orbital, *1s*, with orbits of the electron, which either go directly through the nucleus or come very close to it. However, this orbital is not simulated here. The reason is that doubts arise from the fact that one can calculate nearly exactly the frequency v of the first line of the Lyman series [22] by the simple formula $v=(v_0+ v_1)/3$=2.46743×10^{15} [1/s]. The exact value is $v=c/\lambda$=2.46601×10^{15} [1/s] with λ=121.57 [nm]. This is a relative discrepancy of 5.7×10^{-4}. Here, the quantities v_0 and v_1 are the orbital frequencies of the electron in the innermost two orbits of Bohr's model with v_0=6.57968×10^{15} [1/s] and v_1=0.822413×10^{15} [1/s]. This is also a question that still needs to be clarified.

5.2 Numerical basics

Bohr's model is sufficient for us as a first starting point. Our goal is to study the stability of the innermost circular orbits. We start with a model of the hydrogen atom resting in absolute space, i.e., the proton has the speed v_P = 0 m/s, neglecting the minimal co-motion of the hydrogen nucleus. Our own C-program QuandBed.cpp was used. It uses the plane coordinate system (x, y). All calculated trajectories lie in this plane. The quantity $r=a_0$ is the first orbit radius, i.e., the radius of the innermost orbit in Bohr's model. Because of Puthoff's effect, the relativistic increase of mass of the electron is different than in Bohr's model. Therefore, the starting values of the orbit have changed. The mass of the electron is m_e=9.110110827×10^{-31} [kg], the starting speed of it is v_e=2.187008493×10^6 [m/s]. The distance between the electron and the center of mass is $r=a_0$=5.291772109×10^{-11} [m], the distance electron-proton is r_{ep}=5.294654328×10^{-11} [m]. The circular frequency of the Compton radiation of the proton is ω_{C0}=7.763440649×10^{20} [rad/s], and the relativistically changed circular frequency of the Compton radiation of the electron is ω_{Ce}=7.763853838×10^{20} [rad/s] (by Puthoff's effect). The difference between the two frequencies is ω_{diff}=4.131886828×10^{16} [rad/s], which is nearly the same as the circular frequency of the DeBroglie-wave, i.e., $\omega_{DB} = m_e v^2 / \hbar$ =4.131887051×10^{16} [rad/s].

The Euler-Cauchy method with constant time step dt was used for the integration of the kinematic equations of our model. The Euler-Cauchy method is the simplest method for numerically solving an initial value problem. It does not matter whether there is a simple ODE or a system of ODEs of any order. An ODE of higher order, e.g., of second order, is converted into two ODEs of first order. All ODEs of a system of ODEs are integrated in parallel. Is $y'=f(x)$ the ODE and (y_0, x_0) the initial value, then the numerical solution of the

first integrating step is $y_1=y_0+f(x_0)dx$. The step size dx must be chosen appropriately. To provide the next integrating step, one increases x by $x_1= x_0+dx$. Now, one can perform the next integrating step, i.e., $y_2=y_1+f(x_1)\,dx$, etc. The user controls the accuracy of the solution by the step size.

In the highly compressed flow-chart, Table 2, of the C-program CondBed.cpp, the index *p* means the *proton*, index *e* means the *electron*. Quantity *norbit* is the number of integrated orbitals, *ns* is the number of steps of the integration of one orbital.

Table 2: Highly compressed flow-chart of the C-program *CondBed.cpp*

```
Set  parameter vectors: Radii, colors, beta, …, ns
Set Bitmap: Background color, coordinate cross
Define physical constants, set general initial values

for(iorbit=0; iorbit<norbit; iorbit++) //Loop of orbits
    Set orbital parameters: r, dt, beta, …, ns
    Set orbital initial values: xp0, yp0, xe0, ye0, f0, …

    for(n=0;n<ns;n++) //Loop of integration of ODEs
        Components of force: fpx, fpy, fex, fey
        Components of acceleration: apx, apy, aex, aey
        Integrating components of speed: vpx, vpy, …
        Integrating components of position: xp, yp, ….
        Relativistic correction of mass, Puthoff's effect
        Circular frequencies, Doppler effect
        Pass-on of the wave functions sinp, sine, …
        Calculate new force f
        Set colored point in the bitmap
    End of loop n
End of loop iorbit

Output graphics as bitmap
Please, contact author SvW for the full text of the C-program
```

The distance proton-electron is $\vec{r}_{ep} = \vec{r}_e - \vec{r}_P$. The distance between the center of mass and the electron is $\vec{r}$. Our chosen starting position of the proton is $\vec{r}_P = (-a_0(m_e/m_P), 0)$, that of the electron is $\vec{r}_e = (a_0, 0)$. The starting velocity $\vec{v}_P$ of the proton is $(-v_e(m_e/m_P))$, that of the electron is $\vec{v}_e = (v_e, 0)$.

The emitted waves of the proton and electron were calculated stepwise over time by the addition theorems of sine and cosine. This procedure is immune to phase jumps or a change of the time step *dt* during the integration of the kinematic equations. However, one must set starting values. The wave emitted by the proton starts with $sin_P = 0$ and $cos_P = 1$. The wave emitted by the electron starts with $sin_e = sin(\varphi_e)$ and $cos_e = cos(\varphi_e)$. Hereby, φ_e is the possible phase shift between the waves of the proton and the electron at start. However, in our simulations, $\varphi_e = 0$ was always the case.

The time of one circular orbit of the electron is $T=2\pi\, r/v$. The constant time step *dt* of the integration was calculated by $dt=T/n_s$. The number of steps of the integration, n_s, was set a priori. In most simulations $n_s=10^6$ was used. This number was large enough. Doubling the

number of steps showed only insignificant changes in the results. Starting time was always t = 0.

For the decomposition of the central force (force of attraction) or radial force (centrifugal force) into their x- and y-components, one needs the rotation angle φ_U. It is $sin(\varphi_U)=y_e/r$ and $cos(\varphi_U)=x_e/r$. At the beginning of the simulations, there was no indication of the size of the factors β_p and β_e. Therefore, simulation experiments with the aim of finding a value for the product $\beta=\beta_p\beta_e$ were performed by us. The value chosen was β=0.25. Our only criterion was the stability of the orbit.

The force acting on the electron is $\vec{f}_e = -\frac{e^2\,\vec{r}}{4\pi\,\varepsilon_0\,r^3}\left(1+\beta\sin(\omega^*_{C0}\,t)\sin(\omega_{Ci}\,t)\right)$, the force acting on the proton $\vec{f}_P = -\vec{f}_e$. Hereby, the angular frequency, ω_0, is changed by the Doppler effect (with resting source (proton) and moving observer (electron)), i.e., one obtains $\omega^*_{C0} = \omega_{C0}\left(1-\frac{\vec{v}\,\vec{r}}{r\,c}\right)$. However, at the start, the force f has, because of t=0, the value $f = -e^2/(4\pi\varepsilon_0\,r_{ep}^2)$. By decomposing into components, one obtains $f_x = f\,cos(\varphi_U)$ and $f_y = f\,sin(\varphi_U)$. To be able to calculate the acceleration, we need the momentary relativistic mass of the electron. It is $m_e = m_{e0}(1+2a_e/r_{ep})/\sqrt{1-v^2/c^2}$. So, the acceleration of the electron is $\vec{a}_e = m_e\,\vec{f}$ with components $a_{ex}=m_e f_x$ and $a_{ey}=m_e f_y$. For the proton, we obtain $\vec{a}_p = -m_p\,\vec{f}$ with components $a_{px}=-m_p f_x$ und $a_{py}=-m_p f_y$. One obtains the new speeds of the electron and proton after one step of integration by adding the increments $\vec{a}\,dt$ to the old values, e.g., the new speed of the electron, $v_{ex} \leftarrow v_{ex} + a_{ex}\,dt$, $v_{ey} \leftarrow v_{ey} + a_{ey}\,dt$. Here, the arrow means the replacing of the old value with the new value on the right side. Similarly, one obtains the new coordinates x and y of the proton and electron, e.g., $x_e \leftarrow x_e + v_{ex}\,dt$.

The distance between electron and proton changes by a radial movement. This also changes the relativistic mass of the electron, and, therefore, its Compton angular frequency. It also needs to be updated by the relation $\omega_{Cer} = \omega_{C0}(1+2a_e/r_{ep})$.

The new time after one step of integration is $t \leftarrow t+dt$. The example of the wave emitted by the proton shall illustrate the updating (or pass-on) of the sine and cosine. First, one stores the old values of sin_P and cos_P (e.g. $sin_{P,old} \leftarrow sin_P$). Then, one updates the value of $sin(\omega_{C0D}\,t)$ by the addition theorem: $sin_P \leftarrow sin_{P,old}\,dcos_P + dsin_P\,cos_{P,old}$ with $dsin_P=sin(\omega_{C0D}\,dt)$, and $dcos_P=cos(\omega_{C0D}\,dt)$. In the same way, one updates the cosine, i.e., $cos_P \leftarrow cos_{P,old}\,dcos_P - sin_{P,old}\,dsin_P$.

The new force f after one step of integration is then $f = -(e^2/(4\pi\varepsilon_0\,r_{ep}^2))(1+\beta\,\sin_P\sin_e)$ using the updated values of sin_P and cos_P. With that result, we return to the beginning of the programmed loop, and the next step of integration starts. The coordinates of the orbital curve are stored as points in a pixel graph. The simulation stops after a predefined number of steps with the output of the graphic. The total number of steps defines the number of orbits of the electron.

Fig. 5.a shows the simulated orbitals for 5 different radii.

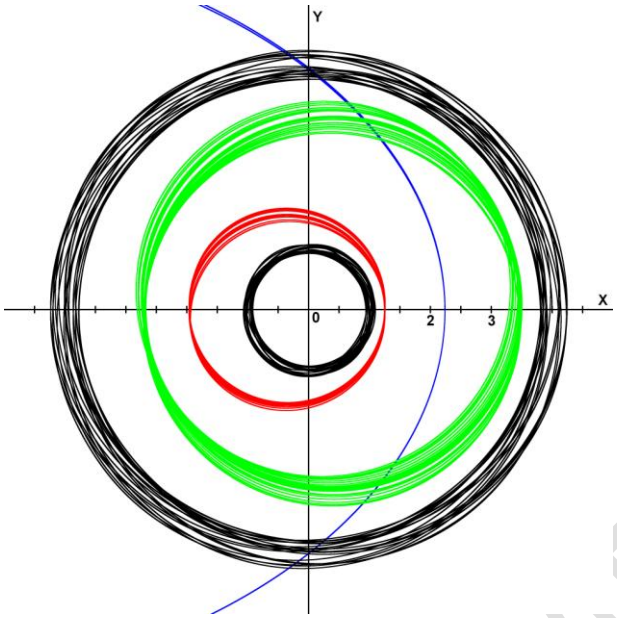

Fig. 5.a: Orbitals for 5 radii

The orbitals of the radius a_0 (innermost black orbital) and of the radius $a_1=4a_0$ (outer black orbital) are assigned to permissible Bohr's orbits. One can see stable, circular, and centered orbitals in the form of tapes with sharp boundaries, and it is clearly to realize that the width of the tapes increases with increasing radius.

The orbitals of the radii 1.25 a_0 (red), 2.24 a_0 (blue), and 3.5 a_0 (green) are orbitals of forbidden radii. One recognizes them by their ellipsoid form and their lateral displacement. The orbital of radius 2.24 a_0 (blue) is completely out of the ordinary. The radius 2.24 a_0 is that for a function $\overline{F}(r)$ that assumes the value of zero, but with a negative derivative (see Fig. 4.a). This orbital has the shape of a great ellipse, only a small part of which can be seen here. These elliptic orbitals arise, because we were unable to find any mechanism in our simulation that would throw the electron under emission of energy out of a forbidden orbit. This is, as indicated above, a question that still needs to be clarified.

A simulation with 100 orbits in each case illustrates the stability and sharp limitation of the tape-shaped orbitals. The two radii used were both permitted Bohr's radii, a_0 (black) and $a_1=4a_0$ (red) (see Fig. 5.b). In the orbital to the radius a_0, the program has drawn a red circle with the radius a_0 as reference. In the orbital to the radius $a_1=4a_0$, the reference circle is black.

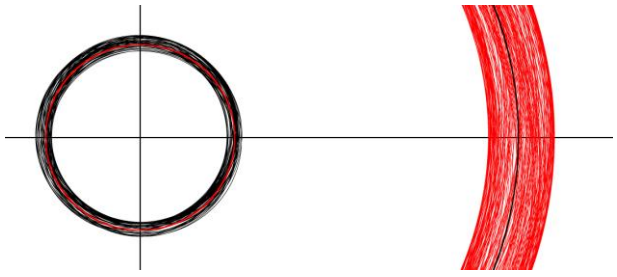

Fig. 5.b: Two permissible orbitals with 100 orbits in each case

In a second simulation, a moving proton was considered. The speed of translation, $\vec{v}_P$, was $v_{px}=369500$ [m/s] and $v_{py}=0$, i.e., the speed of the sun relative to the background microwave

radiation. In Fig. 5.c, the orbits of the electron seen by the proton are circular orbits (black), but the actual path of the electron in the absolute space is formed by a cycloid (red).

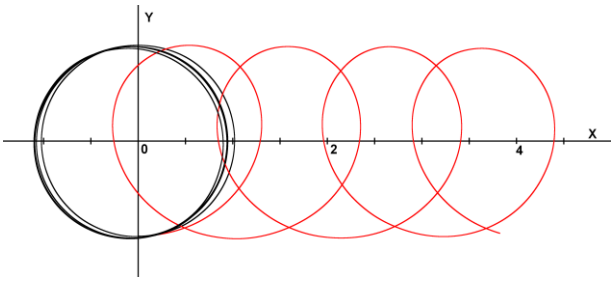

Fig. 5.c: Circles seen by the proton (black), cycloidal trajectory (red) in absolute space

Compared with the case $\vec{v}_P$ =0, our C-program has needed only marginal changes. One reason was that the finite velocity of propagation of the field of the proton was neglected because the speed of the proton, 369 km/s, is small relative to the speed of light.

6. Results and Discussions

The assumption of an absolute space in which waves propagate together with the assumption of the significant speed of 369.5 km/s of the sun and the earth relative to the absolute space make the use of Legendre's spherical functions as done in the QM a very good, but purely mathematical description of the quantum conditions in the atom. Therefore, the authors would like to open a further window of insight to approach the physical cause of the quantum conditions in the atom.

Table 1 shows that the Compton angular frequency of the electron that circles on an allowed Bohr's orbit with principal quantum number *n* indeed deviates to a first approximation by a factor of n of the respective angular frequency ω_{0n} from the Compton angular frequency of the proton. This gives us a clue that indicates that, by way of the relativistic change of mass and the connected change of the frequency of the electron, there exists a connection between the Compton frequency and the orbital frequencies. Unfortunately, the ratios $(\omega_{Cn} - \omega_{C0}) / \omega_{0n}$ are not the integers n=1, 2, 3, but the slightly different values 1.000052, 2.000214, and 3.000685. Here, one could hypothesize a connection to the very small imprecision of the starting value of the simulation of the angular momentum.

Another surprising result is that Bohr's orbits with their strongly fixed radii change to orbitals in the form of sharply limited tapes (see Fig. 5.a and 5.b). This indicates a close relationship between AFM and QM. Adding the influence of the magnetic field of the proton, one would, by the lateral deviation of the electron, obtain a three-dimensional structure that is shaped as a spherical shell. Allowing also elliptical orbits, one surely obtains orbitals which are even more similar to the orbitals known from the QM. By the uncertainty caused by the AFM, and, together with the precession of the orbital planes in the magnetic field of the proton, one would obtain orbitals with probabilities of residence of the electron which would fit very well the orbitals known from the QM.

However, the AFM still raises many questions that need to be clarified. This way, it is only a starting point for the continuing search of the physical cause of the quantum conditions in the atom. The most serious deficiency is that, despite the fact that the zeros of the function $\overline{F}$ (r) (see Fig. 4.a) are positioned at the right places, i.e., at the correct radii of the allowed Bohr's orbits, this fact is not sufficient to establish a quantum condition in the simulation. The model in its momentary state accepts *all* orbits as stable orbits. Only in the cases of forbidden orbits, it produces elliptical orbits instead of circular ones (see Fig. 5.a). However, if one studies the orbital angular momentum *J* of the electron, one finds that it assumes, also in our model, values that are integer multiples of $\hbar$, and that it is stable within a very small range of variation. In our model, the values of $J_n/\hbar = m_e v_n r_n/\hbar$ have the starting values 1.000027, 2.000013, and 3.0000089 for n=1, 2, 3. The values of $J_n/\hbar$ vary slightly during the simulation of an orbit, however, they remain within the limits of the inaccuracy of the starting value.

To fix the values of the angular momentum at an integer multiple of $\hbar$ on an allowed Bohr's orbit, we made experiments with an algorithm that radiates wave energy to the environment or collects energy from it. However, on the allowed Bohr's orbits, no change in the calculated ribbon shaped orbitals was found. Also, the experiment to leave a disallowed orbit in the direction of an allowed orbit under energy transfer was not feasible, because the orbit spiralled out of control. Otherwise, we did not wish to construct a forward-thinking algorithm using integral data, because of our belief that physics works exactly at the position of the electron. Therefore, one should only use the momentary kinetic data of the electron, i.e., energy, momentum, and the acting forces. But these considerations are goals of quantum electrodynamics (QED) that go beyond the aim of the present study [23, 24].

In this study, the *1s* orbital of the QM was not considered. This spherical orbital describes electrons on paths that cross the nucleus or are located, at the least, near the nucleus, and have no angular momentum. The Stern-Gerlach experiment with neutral silver atoms is seen as a proof of the existence of this orbital. As a reason for our disregard, one can consider the ratios of the orbital frequencies F_{ui} and F_{uj} to the frequency F_{ij} of the emitted wave during the change of the orbitals. Here, one finds that a relatively exact prediction of the frequency F_{ij} can be reached by combining the orbital frequencies F_{ui} and F_{uj} in a simple formula. The frequencies F_{ij} were calculated by us using the differences in the energy levels. Here, the number *i* is the principal quantum number of the orbital of a series that exhibits the deepest energy level, and $j=i+1$ the next higher energy level. The first six series of the H-atom are *Lymann, Balmer, Paschen, Bracket, Pfund,* and *Humphreys*. Table 3 shows the line of the series with the longest wavelength. The emitted frequencies, $F_{ij,E}$, were calculated with the formula $F_{ij,E} = (E_j - E_i)/h$ using the energy levels of the seven deepest Bohr's orbits. The seven pairs of orbital frequencies, F_{ui} and F_{uj}, were also calculated using Bohr's theory. Our formula of prediction is

$$F_{ij}^{*} \approx (F_{ui} + F_{uj})/(2 + 1/((j-1)^2 - (i-1)^2)\,. \quad (6.1)$$

The relative error is $error = \left| (F_{ij}^{*} - F_{ij,E})/F_{ij,E} \right|$ (or *error*% = *error* ·100%, respectively).

Table 3: Line, wavelength observed, frequency calculated, frequency estimated, and error.

Line $j \rightarrow i$	λ [nm]	$F_{ij,E}$	est. F_{ij}^{*}	error %

Lymann 2→1	121.57	2.4674×10^{15}	2.4674×10^{15}	0.0024
Balmer 3→2	656.3	4.5527×10^{14}	4.5736×10^{14}	0.46
Paschen 4→3	1875	1.6157×10^{14}	1.5798×10^{14}	2,22
Bracket 5→4	4051	7.3943×10^{13}	7.2539×10^{13}	1,90
Pfund 6→5	7460	3.9894×10^{13}	3.9426×10^{13}	1.17
Humphr. 7→6	12370	2.4443×10^{13}	2.3821×10^{13}	2.55

The averaged geometric error of the series 2 to 6 is 1.42%. However, the transition of the Lyman series from the principal quantum number 2 to 1 has a very small error of 0.000024 or 0.0024%, respectively. This deviation is smaller than the deviation of 0.05% between observation and calculation) [22] and gives our estimation formula some weight. Since the Lyman series is the series of the hydrogen atom with the shortest wavelength, we miss, considering the known lines, the transition from the principal quantum number 1 to 0. For the principal quantum number 0, no orbital frequency exists based on the chaotic orbits near the nucleus. Therefore, our formula of prediction is not usable in this case, and the authors consider the existence of the *1s* orbital a question that still needs to be clarified.

By the interference of the alternating field of the proton and the electron, waves arise on Bohr's orbits matching the DeBroglie-waves of the moving electron. However, thus far, the DeBroglie-waves has been considered by us as artifacts in our model. There are two reasons. The first reason is that the addition of the DeBroglie-waves into our simulation has not produced any improvement. The second reason is that it is not clear to us whether DeBroglie-waves of free electrons really exist, or are only artifacts in the sphere of influence of the alternating field of the proton. The authors, again, consider this a question that still needs to be clarified.

7. Conclusions

The study deals with the origin of the quantum conditions. The assumption of Newton's absolute space together with the speed of 369.5 km/s of the sun leads to cycloidal or helical orbits of the electron around the proton. This kind of orbits is a previously unnoticed fact and not compatible with the model of a closed circular standing wave. It was the aim of this study to search for alternative models.

The possibility given by the AFM to calculate orbits and orbitals of an electron should encourage us to seek a programmable algorithm for the emission or catching of a photon. Naturally, it would be helpful to have a model of the photon, but it is unlikely that, in the foreseeable future, such a model will be available. So, creativity will be required at this point. The idea that electrons move themselves down from a higher orbit to an orbit with a lower level of energy suggests, however, the idea that the single photon must not have a constant frequency over its spatial extension. Only a properly-chosen average can represent the emitted frequency, and only for a great number of single photons created by stimulated emission in the correct phase, one will find a wave field with narrow width of the line.

8. Summary

The assumption of an absolute space together with the speed of 369.5 km/s of the sun relative to this absolute space leads to cycloidal or helical orbits of the orbiting electron. This makes the use of Legendre's spherical harmonics in the QM a purely mathematical formalism for the description of the quantum conditions in the atom. However, we are looking for the physical bases of the quantum conditions. The good news is that the cycloid and the helix are curves composed from a circular and a translational motion. Therefore, decomposition is possible of the total energy into rotational and translational energy. Also, the decomposition of the momentum and angular momentum is well possible for both curves. So, it will be very likely that the mathematical results of the QM will not change. Only the physical foundation of the quantum conditions would change, a question which merely falls in the sphere of natural philosophy.

The AF-model, new in the context of the QM, assumes the existence of alternating fields for both the proton and the electron. The energy comes from the Higgs-field, as also the energy of the synchrotron radiation which is very weak due to the small speed of the electron [3]. By Puthoff's relativistic effect, as an adaptation from the theory of gravitation, the electron changes its relativistic mass and, thus, its Compton frequency. This adaptation is a new and important brick of the AF-model. By the interference of the alternating fields of the proton and the electron, beats are caused which are on Bohr's circular orbits integer multiples of the orbital frequency ω_0. However, this also means that, on Bohr's circular orbits, in a first approximation, one can calculate the electrostatic force between electron and proton in the same way as without the existence of the alternating fields. However, in a second approximation, disturbances arise that stem from the fact that, on Bohr's orbits as well, the electrostatic forces are constant only on average. These disturbances are the cause of orbitals instead of sharp orbits, i.e., in our simulations, the broadening of the circular orbits into ribbon-shaped orbitals.

The AFM allows one to calculate Bohr's circular orbits as ribbon-shaped orbitals. Otherwise, in its momentary state, the AFM allows one to also calculate stable orbitals on disallowed radii. A positive result is that the illegal orbitals have an elliptic, not a circular shape. Also, the magnetic field of the proton was not used in any way. It could be important to ensure a stable orientation of the coordinate system in a physical way. Only then, the term *orbit* would obtain some sense.

Questions that still need to be clarified include: (1) De Broglie-waves, are they real or are they only artifacts of the interaction of the alternating fields of electron and proton? (2) Does the 0-th orbital of the QM exist, and if it does, how should it become manifest in the AFM? (3) Is it possible to find a programmable algorithm that can simulate the emission or the catching of a photon, or, in other words, what brings the electron from a disallowed orbit to an allowed one by the emission of a photon? However, this question and the important question concerning the interaction of the Higgs-field with the proton and the electron concerns QED and goes beyond the aim of this study.

Authors' contributions

This work was carried out in collaboration between both authors. Both authors read and approved the final manuscript.

References

[1] Wichmann E. *Quantenphysik*. Springer, ISBN 3-540-41572-6 (2001)

[2] Feinman R. et. al., Feynman-Vorlesungen über Physik, De Gruyter, ISBN-13 978-3110355468 (2015)

[3] Hofmann A. The physics of synchrotron radiation, Cambridge University Press, ISBN 0-521-30826-7 (2004)

[4] Breit G. An interpretation of Dirac's Theory of the electron, Proc. Nat. Acad. Sc., **14** (7), 1928, pp. 553-559, doi: 10.1073/pnas.14.7.553
Breit An Interpretation of Dirac's Theory of the Electron

[5] Schrödinger E. Über die kräftefreie Bewegung in der relativistischen Quantenmechanik: Aus den Sitzungsberichten der Preußischen Akademie der Wissenschaften Phys.-Math. Klasse, Band **24**, 1930 Schrödinger 1930 kräftefreie Bewegung

[6] Nave R. "Quarks". HyperPhysics. Georgia State University, Department of Physics and Astronomy. Retrieved 29 June 2008. Nave, R. (2008) Quarks. HyperPhysics. Georgia State University, Department of Physics and Astronomy, Atlanta. - References - Scientific Research Publishing (scirp.org)

[7] Bohr N. On the constitution of atoms and molecules part I, Philosophical Magazine **26** (1913) pp. 1-25 Niels Bohr, On the Constitution of Atoms and Molecules, Part I - PhilPapers

[8] Bohr N. The spectra of helium and hydrogen, Nature **92** (1914) pp. 231-232 doi:10.1038/092231d0 Bohr 1914 The Spectra of Helium and Hydrogen | Nature

[9] Sommerfeld A. Zur Quantentheorie der Spektrallinien (I+II), Ann. Phys. **51** (1916) pp. 1-94 Sommerfeld Zur Quantentheorie der Spektrallinien

[10] Dirac P A M. Principles of quantum mechanics, 4. Auflage, Oxford University Press, (1958) ISBN 0-19-851208-2

[11] Schrödinger E. Quantisierung als Eigenwertproblem, Ann. Phys. **79** (1926) pp. 361-376 Schrödinger Quantisierung als Eigenwertproblem

[12] Demtröder W. Experimentalphysik 3, 5. Springer ISBN. 978-3-662-49093-8 (2005)

[13] von Weber S, von Eye A. Two-way and One-way Vacuum Speed of Light under the Membrane Paradigm, Phys. Sci. Int. J. Vol. 2017; **15**(2): 1-17.
http:Two-way and One-way Vacuum Speed of Light under the Membrane …

[14] Becker K., Becker M., Schwarz J. String theory and M-theory: A modern introduction. Cambridge University Press. ISBN 978-0-521-86069-7 (2007)

[15] Horowitz GT, Strominger A. Black strings and p-branes. Nucl. Phys. B 1991; **360**; 197–209, Black strings and p-branes - ScienceDirect.

[16] Randall L, Sundrum R., An Alternative to Compactification. Phys. Rev. Lett. 1999; **83**: p. 4690 https://journals.aps.org/prl/abstract/10.1103/PhysRevLett.83.4690

[17] von Weber S, von Eye A. Mass under the Membrane Theory of Gravitation, Phys. Sc. Int. J. Vol. 2022; **26**(3): 25-38; PSIJ.89400 ISSN: 2348-0130 https://doi.org/10.9734/psij/2022/v26i330314

[18] Chandrasekhar S. An introduction to the study of stellar structure. 1939

[19] Perkins D H. Introduction to high energy physics, Cambridge University Press, 2000 ISBN 0-521-62196-8

[20] Puthoff HE. Polarizable-Vacuum approach to GR. Found. of Physics. 2002; **32** (6):1-24 . https://arxiv.org/ftp/gr-qc/papers/9909/9909037.pdf

[21] von Weber S, von Eye A. Geodetic Precession under the Paradigm of a Cosmic Membrane. Phys. Sc. Int. J. Vol. 2016; **10** (4):1-14. prh.sdiarticle3.com/review-history/14928

[22] Kramida A., Ralchenko Yu., Reader J., and NIST ASD Team. NIST Atomic Spectra Database (ver. 5.7.1), https://physics.nist.gov/asd (2020)

[23] Guralnik G. "The History of the Guralnik, Hagen and Kibble development of the Theory of Spontaneous Symmetry Breaking and Gauge Particles". International Journal of Modern Physics A 24 (14): 2601–2627. [0907.3466] The History of the Guralnik, Hagen and Kibble development of the Theory of Spontaneous Symmetry Breaking and Gauge Particles (arxiv.org) (2009)

[24] Mandl F, Shaw G. Quantenfeldtheorie, Aula-Verlag, Wiesbaden, (1993) ISBN 3-89104-532-8